

Application of Gramian and Focusing Structural Constraints to Joint Inversion of Gravity and Magnetic Data

M. Jorgensen^{1,2}, M. Zhdanov^{1,2}

¹ Consortium for Electromagnetic Modeling and Inversion, University of Utah; ² TechnoImaging

Summary

We develop and compare two methods of jointly inverting airborne gravity gradiometry (AGG) and total magnetic intensity (TMI) data in the presence of remanent magnetization. One is based on Gramian structural constraints, and the other uses a joint focusing stabilizer. Enhancing structural similarity between multiple geophysical models can help isolate mineralized targets. In the areas with remanent magnetization, one should invert not only for magnetic susceptibility, but for a 3D distribution of magnetization vector as well. The Gramian structural constraints enforce the correlation of the model gradients. The joint focusing stabilizer is implemented using minimum support approach, which forces a similarity of the shapes of the targets. We apply these novel joint inversion methods to interpretation of the airborne data collected over the Thunderbird V-Ti-Fe deposit in Ontario, Canada. By combining the complementary AGG and TMI data, we generate the jointly inverted models which provide a more consistent image of the geologic structure of the area.

Introduction

Structural constraints based on a correlation of model parameters or model gradients (Gallardo and Meju, 2003) have proven to be an effective tool for joint inversion. We present two novel approaches to addressing this problem. The first approach is joint inversion with Gramian structural constraints (Zhdanov et al., 2012; Zhdanov, 2015), enforcing correlation of the gradients of density and magnetization models. The second approach is joint inversion with a joint focusing stabilizer (Molodtsov and Troyan, 2017), enforcing model sparsity via a modified minimum support constraint (Zhdanov, 2015).

Geologic interpretation of multimodal geophysical models inverted from potential field data can be also complicated by the presence of remanent magnetization. We present a method of accounting for remanent magnetization based on inverting magnetic data for magnetization vector, as opposed to magnetic susceptibility. This approach, however, introduces more degrees of freedom into the inversion and increases non-uniqueness. We overcome this problem by jointly inverting AGG and TMI data sets.

As an illustration of these approaches, we present the results of inverting the AGG and TMI data collected over the Thunderbird V-Ti-Fe deposit in Ontario, Canada. These data were gathered in a project collaboratively operated between the Ontario Geological Survey (OGS) and the Geological Survey of Canada (GSC). The survey was flown with the Fugro Airborne Surveys gravity gradiometer and magnetic system between 2010 and 2011. We present the density and magnetization vector models of the Thunderbird deposit obtained from standalone, Gramian, and joint focusing inversions.

Gramian joint inversion

The geophysical inverse problem is formulated by the operator equations $m^{(i)} = (A^{(i)})^{-1}d^{(i)}$, ($i = 1,2$), where $m^{(1)} = \rho$ is the density model, $m^{(2)} = \{M_x, M_y, M_z\}$ are the models corresponding to the scalar components of magnetization vector, $A^{(i)}$ are the forward modelling operators, $d^{(i)}$ are the data, and the superscript $i = 1,2$ indicates the gravity and magnetic problems, respectively. The inverse problem is ill-posed, so we apply the regularization and optimize a parametric functional using the conjugate gradient method (Zhdanov 2009; 2015).

Separate misfit and stabilizing terms, corresponding to the AGG and TMI data, are combined in the joint parametric functional and subject to the Gramian constraint:

$$P = \sum_{i=1}^2 \varphi(m^{(i)}) + \alpha \sum_{i=1}^2 s(m^{(i)}) + \beta G(\nabla m^{(i)}) = \min. \quad (1)$$

The misfit terms are defined as follows,

$$\varphi(m^{(i)}) = \left\| W_d^{(i)} (A^{(i)}(m^{(i)}) - d^{(i)}) \right\|_2^2, \quad (2)$$

where $W_d^{(i)}$ are the data weights, $A^{(i)}(m^{(i)})$ are the predicted data, and $d^{(i)}$ are the observed data. The stabilizing terms are defined as follows,

$$s(m^{(i)}) = \left\| W_m^{(i)} (m^{(i)} - m_{apr}^{(i)}) \right\|_2^2, \quad (3)$$

where $W_m^{(i)}$ are the model weights and $m_{apr}^{(i)}$ are the a priori models. The Gramian term, which enforces structural similarity, is given by the following formula,

$$G(\nabla m^{(i)}) = \sum_{\gamma=x,y,z} \begin{vmatrix} (\nabla m^{(1)}, \nabla m^{(1)}) & (\nabla m^{(1)}, \nabla M_\gamma) \\ (\nabla M_\gamma, \nabla m^{(1)}) & (\nabla M_\gamma, \nabla M_\gamma) \end{vmatrix}, \quad (4)$$

where $\nabla m^{(1)}$ are the gradients of the density model, ∇M_γ are the gradients of the scalar components of magnetization vector, and $(*,*)$ denotes the inner product (Zhdanov, 2015). As this determinant is minimized, the model gradients are aligned enforcing structural similarity.

Joint focusing inversion

Separate misfit terms, corresponding to the AGG and TMI data, are combined in the joint parametric functional and subject to the joint minimum support constraint:

$$P = \sum_{i=1}^2 \varphi(m^{(i)}) + \alpha s_{jf}(m^{(i)}). \quad (5)$$

The misfit terms are defined in (2). We invert for all components of magnetization vector; however, only the vertical component, $m_z^{(2)} = M_z$, is incorporated into the focusing stabilizer. The joint focusing term is defined as follows,

$$s_{jf}(m^{(i)}) = \iiint_V \frac{\sum_{i=1}^2 W_m^{(i=1(2))} (m_z^{(i=1(2))} - m_{z,apr}^{(i=1(2))})^2}{\sum_{i=1}^2 W_m^{(i=2(1))} (m_z^{(i=2(1))} - m_{z,apr}^{(i=2(1))})^2 + e^2} dv, \quad (6)$$

where e is the focusing epsilon. Based on standalone inversion results, the vertical component of magnetization vector is dominant, thus the focusing term incorporates density and the vertical component of magnetization vector only to reduce non-uniqueness.

Data and model weighting

Both AGG and TMI data are weighted by a function of the errors:

$$W_d^{(i)} = 1 / (err_f^{(i)} d^{(i)} + err_{abs}^{(i)}), \quad (7)$$

where $err_f^{(i)}$ are the fractional errors (0.05 for the AGG and TMI data), and $err_{abs}^{(i)}$ are the absolute error floors (2-4 Eotvos for the AGG data and 100 nT for the TMI data). Data weights are then further scaled in the joint inversion such that the first misfit for each term $\varphi(m^{(i)})$ is equal to 1. Model weights are determined by the following function of integrated sensitivity:

$$W_m^{(i)} = diag \sqrt[4]{F^{(i)*} F^{(i)}}, \quad (8)$$

where $F^{(i)}$ is the Fréchet derivative of $A^{(i)}(m^{(i)})$, and $F^{(i)*}$ is the complex conjugate. Model weights are then further scaled in the joint inversion by normalizing by the maximum value of the model parameters obtained from standalone inversions.

The regularization terms α, β are adaptively reduced to ensure stable convergence (Zhdanov, 2009; 2015). The inversions are all halted when the χ^2 fit corresponding to both misfit terms drops to 1, meaning we have reached the interpreted noise level.

Results

We inverted the data collected over the Thunderbird deposit shown in Figure 1. Based on potential field data and limited core drilling, Thunderbird is assumed to be a semi-massive V-Ti enriched magnetite with a rough volume of 0.32 km³. TMI data were filtered to eliminate responses from the deeper sources. We inverted the data on a 50x50 m horizontal grid with a logarithmic depth discretization ranging from 25-150 m. Total grid size was ~250,000 cells. The inversions were run on a 16-core Intel Xeon desktop with 128 GB memory. Total runtime was ~10 minutes for the standalone AGG inversion, ~5 minutes for the standalone TMI inversion, ~45 minutes for the Gramian joint inversion, and ~15 minutes for the joint focused inversion.

It can be challenging to resolve both a geologically meaningful magnetic susceptibility model and a good data fit underlying such a narrow, high-contrast (~1000+ nT) anomaly as that in Panel 1(B) (Zhdanov and Cuma, 2018). Inversion for magnetization vector introduces more degrees of freedom in the inversion; however, that also increases the potential for non-uniqueness, which we remedy with joint inversion.

We contrast the standalone inverted models with the jointly inverted models (Figure 2), which have sharper boundaries and more structural correlation, while maintaining the same level of data misfit as the standalone inversions ($\chi^2 = 1$). The inducing magnetic field direction is shown in Panels 2(B), 2(D), and 2(F), for reference with the inverted magnetization vectors.

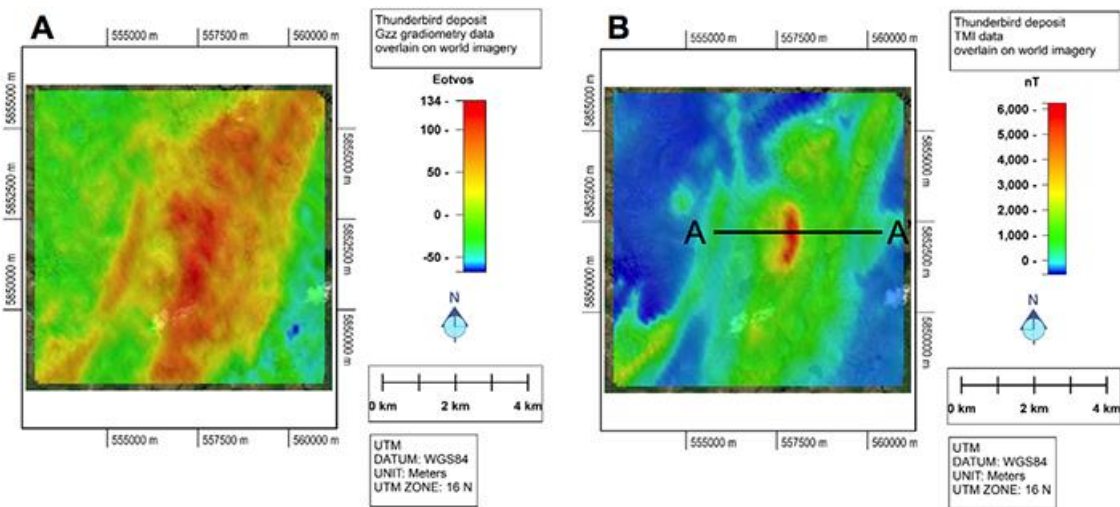


Figure 1 Panel (A) shows the G_{zz} component of the observed AGG data shown in UTM coordinates. Panel (B) shows the observed TMI data map. Profile line AA' is shown in black.

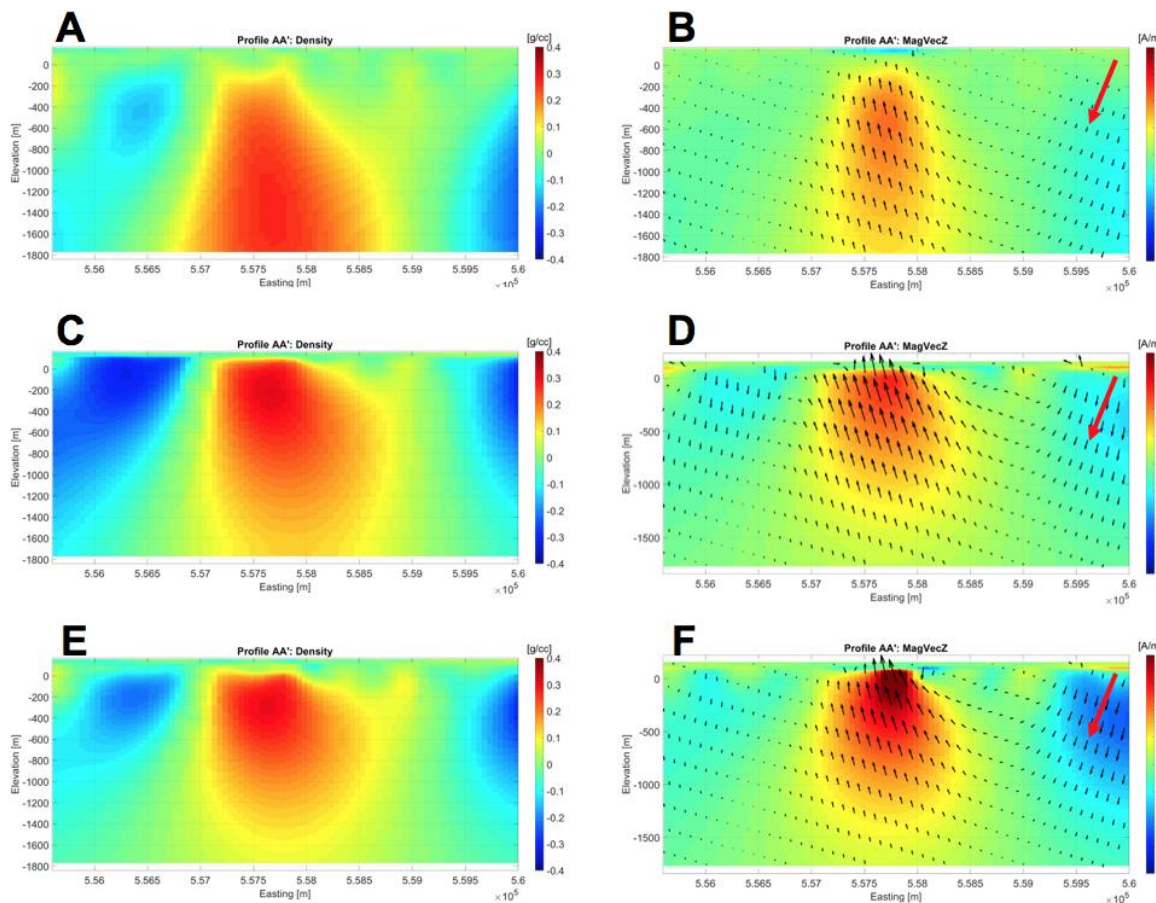


Figure 2 Panels (A) & (B) show vertical sections of the standalone inverted density and magnetic vector models, respectively. Panels (C) & (D) show vertical sections of the Gramian joint inverted density and magnetic vector models, respectively. Panels (E) & (F) show vertical sections of the joint focused inverted density and magnetic vector models, respectively. The color map in panels (B), (D), and (F) is the vertical component of magnetic vector, the black arrows are the full magnetic vector, and the red arrows in the upper right corner indicates the direction of the inducing field.

The cross plots of density and magnetic vector shown in Figure 3 indicate the level of structural correlation. The Gramian joint inversion shown in Panel 3(B) achieves the highest level of correlation, where lineaments corresponding to background and anomaly are clear; however, the joint focused inversion also achieves a high level of correlation and is computationally fast.

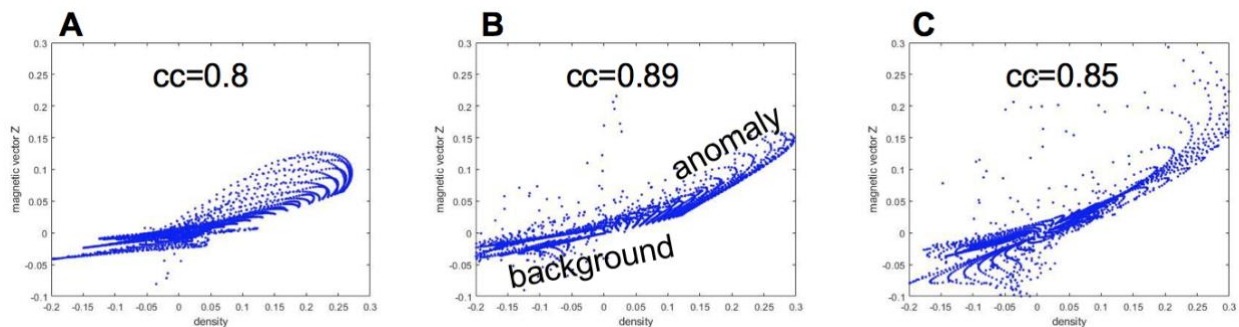


Figure 3 Panel (A) - (C) show property cross plots of density and the vertical component of magnetization vector for the standalone, Gramian, and joint focused inverted models, respectively. The correlation coefficient for each inversion type is denoted cc .

Conclusions

We have introduced the novel methods of joint inversion of AGG and TMI data in the presence of remanent magnetization using both Gramian and joint focusing structural constraints. As an illustration of the developed methods, we have jointly inverted AGG and TMI data gathered over the Thunderbird V-Ti-Fe deposit. The comparison of the standalone inverted density and magnetic vector models versus the joint inverted models demonstrates that the jointly inverted models can recover the more compact bodies with more structural correlation than the standalone inverse solutions, while achieving a similar level of data misfit.

Acknowledgements

The authors would like to thank CEMI and TechnoImaging for the support of this research. The AGG and TMI data were collected by Fugro and made available by the Ontario Geological Survey, Canada.

References

- Gallardo, L.A. and Meju, M.A. [2003]. Characterization of heterogeneous near-surface materials by joint 2D inversion of DC resistivity and seismic data. *Geophysical Research Letters*, **30**(13), 1658.
- Molodtsov, D. and Troyan, V. [2017]. Multiphysics joint inversion through joint sparsity regularization. *SEG Technical Program Expanded Abstracts*, **2017**, 1262-1267.
- Zhdanov, M.S. [2009]. *Geophysical Electromagnetic Theory and Methods*. Elsevier.
- Zhdanov, M.S. [2015]. *Inverse Theory and Applications in Geophysics*. Elsevier.
- Zhdanov, M.S. and Cuma, M. [2018]. Joint inversion of multimodal data using focusing stabilizers and Gramian constraints. *SEG Technical Program Expanded Abstracts*, **2018**, 1430-1434.
- Zhdanov, M.S., Gribenko, A.V. and Wilson, G. [2012]. Generalized joint inversion of multimodal geophysical data using Gramian constraints. *Geophysical Research Letters*, **39** (9).